

# A PARAMETRIC STUDY ON POSITION WORKSPACE CAPABILITY OF CAPAMAN

Gianni Castelli, Erika Ottaviano and Marco Ceccarelli  
LARM: Laboratory of Robotics and Mechatronics  
DiMSAT, University of Cassino  
Via Di Biasio 43, 03043 Cassino (Fr), Italy  
e-mail: g.castelli/ottaviano/ceccarelli@unicas.it

## Abstract

*A parametric study of main workspace characteristics is presented to describe CaPaMan capability and to investigate design effects of its parameters. Several numerical evaluations are reported to cover a wide range of design possibilities, which can help a designer or user to select the optimal solution as function of application peculiarities.*

**Keywords:** Robotics, Workspace, Parallel manipulators, Design of manipulators.

## 1. INTRODUCTION

A parallel manipulator consists of fixed and moving platforms, which are connected by means of several legs operating in parallel. In the last two decades several parallel architectures have been proposed and many prototypes have been built and tested. Parallel manipulators have been proposed as mechanical architectures, which can overcome the limitations of serial robots. The main characteristics and advantages, with respect to open-chain manipulators, can be recognized as greater stiffness, better accuracy and larger payload.

Great attention has been addressed to the evaluation of design and operation performances and several analyses have been carried out through suitable specific or general procedures. Recently great attention has been addressed to the evaluation of workspace capability as a function of design parameters. In particular, an optimization of the manipulator workspace is one of the most important issues because the workspace determines geometrical limits on the manipulation that can be performed by the robot. Some authors have attached the problem of synthesis of parallel manipulators by using a workspace determination that is often based on a discretization, as in [1-2], or its boundary evaluation, as in [3]. Different performance criteria for design purposes take into account the condition number of the Jacobian matrix, as proposed in [4-5] or singularities, [6].

In this paper, we present a parametric study on position workspace capability for the CaPaMan (Cassino Parallel Manipulator), a 3-degree of freedom spatial parallel manipulator, in order to understand

the effect of design parameters on main position workspace characteristics. The position workspace is a set of reachable positions by a reference point in a Cartesian coordinate frame and it gives the positioning capability of a robot. A fairly general algorithm has been used in order to evaluate numerically position workspace characteristics. The parametric study has been carried out by taking into account several different values for each specific design of the CaPaMan robot. Main results have been reported in order to characterize the mechanical design and operation of CaPaMan.

## 2. CAPAMAN (CASSINO PARALLEL MANIPULATOR) AND ITS WORKSPACE CHARACTERISTICS

CaPaMan (Cassino Parallel Manipulator) is a 3-DOF spatial parallel manipulator, which has been conceived and built at LARM: Laboratory of Robotics and Mechatronics in Cassino, Italy, [7], Fig. 1 and Table 1. It is composed by a fixed platform FP that is connected to a movable platform MP by means of three legs, Fig.1a). Each of these legs is composed by an articulated parallelogram AP, a prismatic joint SJ, and a connecting bar CB. CB may translate along the prismatic guide of SJ keeping its vertical posture while the BJ allows the MP to rotate in the space. Each AP plane is rotated by  $\pi/3$  with respect to the neighbouring one. A built prototype is shown in Fig.1b).

Design parameters of a k-th leg mechanism ( $k = 1, 2, 3$ ) are identified through:

- $a_k$ , which is the length of the frame link;

- $b_k$ , which is the length of the input crank;
- $c_k$ , which is the length of the coupler link;
- $d_k$ , which is the length of the follower crank;
- $h_k$ , which is the length of the connecting bar.

The kinematic variables are:

- $\alpha_k$ , which is the input crank angle actuated by a DC motor, as variable from the value  $\alpha_k$  min to  $\alpha_k$  max;

- $s_k$ , which is the stroke of the prismatic passive joint with range from  $s_k$  min to  $s_k$  max.

The size of MP and FP are given by  $r_p$  and  $r_f$ , respectively, where H is the center point of MP, O is the center point of FP,  $H_k$  is the center point of the k BJ, and  $O_k$  is the middle point of the frame link  $a_k$ . MP is driven by the three leg mechanisms through the corresponding articulation points  $H_1, H_2, H_3$ .

The determination of the position workspace and Euler angles can be carried out by using the following expressions [7],

$$x = \frac{y_3 - y_2}{\sqrt{3}} - \frac{r_p}{2}(1 - \sin \phi) \cos(\psi - \theta)$$

$$y = y_1 - r_p(\sin \psi \cos \theta + \cos \psi \sin \phi \sin \theta) \quad (1)$$

$$z = \frac{z_1 + z_2 + z_3}{3}$$

and

$$\theta = \sin^{-1} \left[ 2 \frac{y_1 + y_2 + y_3}{3r_p(1 + \sin \phi)} \right] - \psi$$

$$\psi = \tan^{-1} \left[ \sqrt{3} \frac{z_3 - z_2}{2z_1 - z_2 - z_3} \right] \quad (2)$$

$$\phi = \cos^{-1} \left[ \pm \frac{2}{3r_p} \sqrt{z_1^2 + z_2^2 + z_3^2 - z_1 z_2 - z_2 z_3 - z_1 z_3} \right]$$

( $z \geq z_1 \Rightarrow +$ ;  $z < z_1 \Rightarrow -$ )

when the input motion by  $\alpha_k$  for the legs is given by

$$y_k = b_k \cos \alpha_k$$

$$z_k = b_k \sin \alpha_k + h_k \quad (3)$$

Table 1. Sizes and motion parameters of the built prototype for CaPaMan in Fig 1.

$a_k$	$b_k$	$c_k$	$d_k$	$h_k$	$r_p$	$\alpha_k$ min	$\alpha_k$ max	$s_k$ min	$s_k$ max
[mm]	[mm]	[mm]	[mm]	[mm]	[mm]	[deg]	[deg]	[mm]	[mm]
200	80	100	250	45	135	-50	50		

Position workspace can be determined by considering all reachable points as function of input motion through a scanning process. Figure 2 shows a

3-D representation with Cartesian projections of workspace position. In this figure it is possible to appreciate the dimensions limit of workspace position. Figure 3 shows some workspace cross sections and Fig. 4 shows the relative cross sections dexterity map of CaPaMan.

Figure 5 show the numerical CAD reconstruction of the position workspace. In this figure it is possible to appreciate the shape of whole workspace, not easy to recognize by a points representation like Figs. 2 and 3.

Several applications of the CaPaMan manipulator have been investigated at LARM to use it as earthquake simulators, as robot wrists and in mechanized assembly. In particular several experimental results have been successfully validated the CaPaMan manipulator as earthquake test-bed simulator [8].

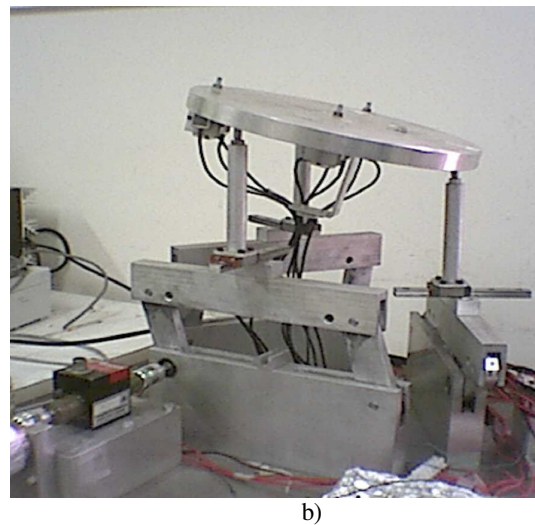
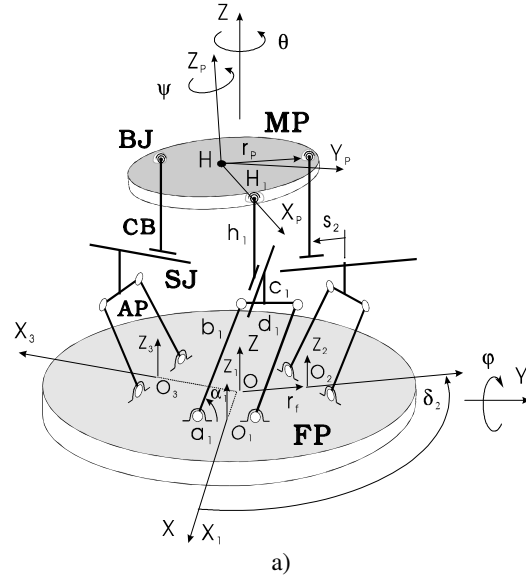


Fig. 1. CaPaMan (Cassino Parallel Manipulator):  
a) a sketch for kinematic chain and design

parameters; b) a built prototype of CaPaMan at

LARM.

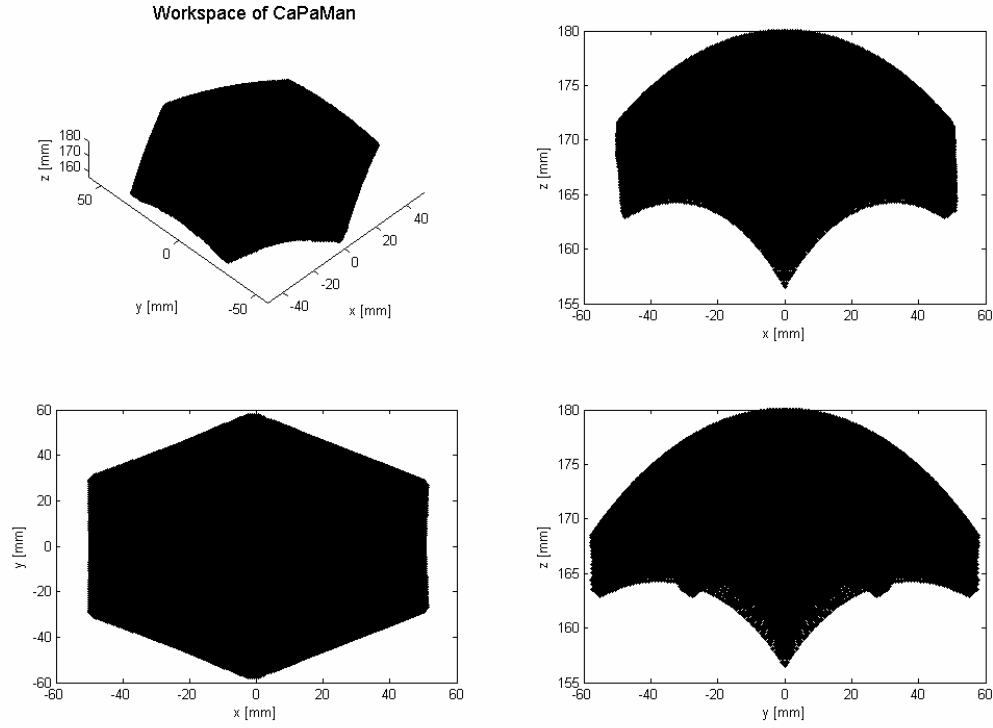


Fig. 2. A 3-D representation with Cartesian projections position workspace of CaPaMan (Cassino Parallel Manipulator) with data in Table 1.

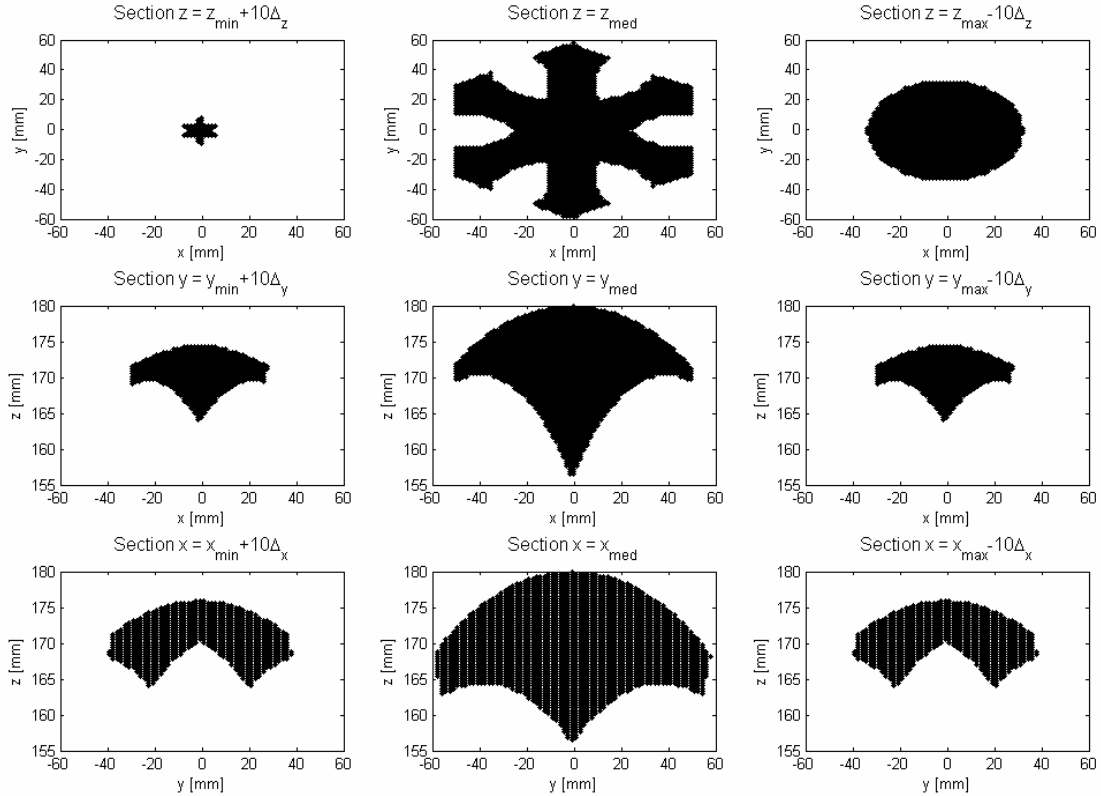


Fig. 3. Workspace cross sections of CaPaMan (Cassino Parallel Manipulator) with data in Table 1.

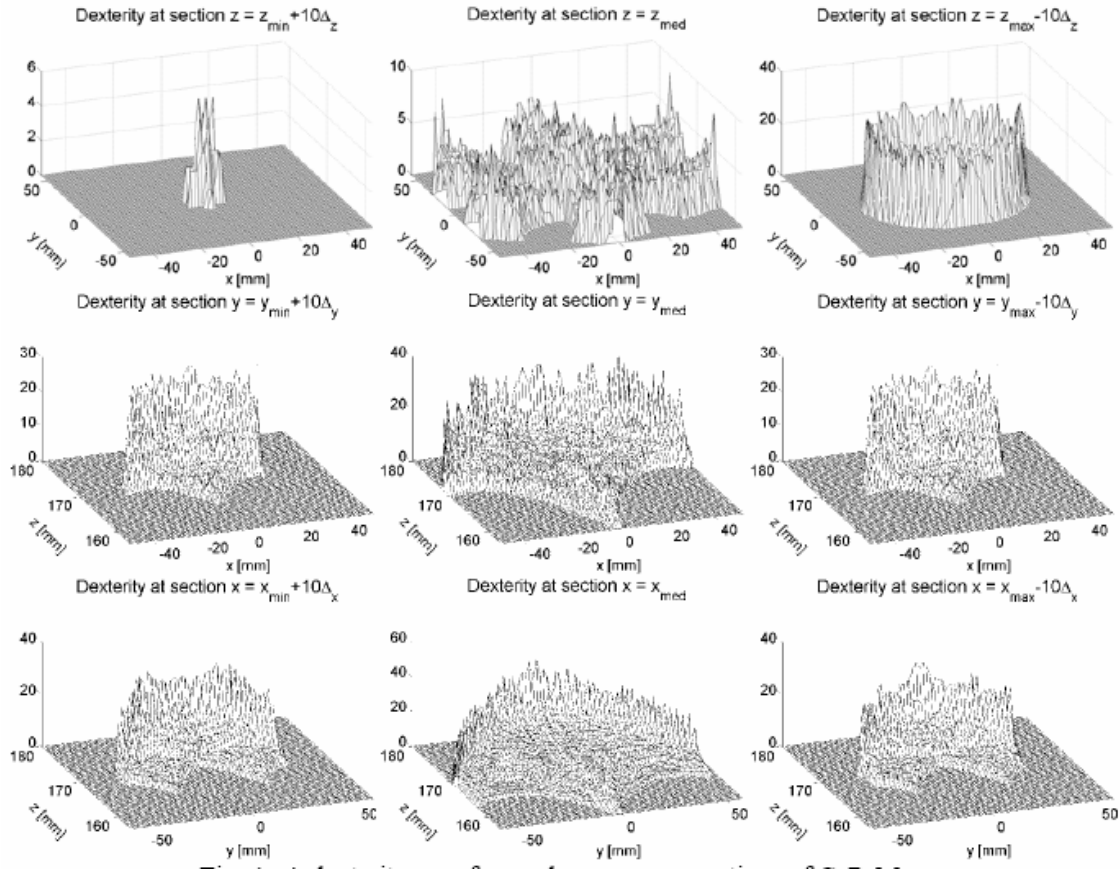


Fig. 4. A dexterity map for workspace cross sections of CaPaMan (Cassino Parallel Manipulator) in Fig. 3 with data in Table 1.

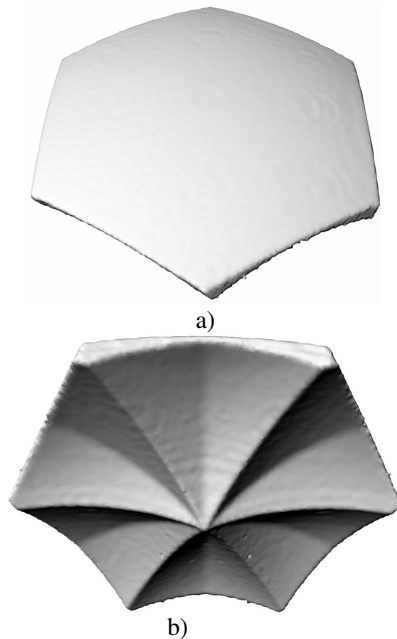


Fig. 5. A numerical reconstruction of 3D workspace of Robot CaPaMan with data in Table 1:

a) front-top view; b) left-bottom view.

### 3. AN ALGORITHM FOR POSITION WORKSPACE ANALYSIS

In this paper, a discretization method is used to determine the position workspace of the CaPaMan [9], which guarantees that all kinematic constraints are taken into account during the computation of the workspace. The algorithm is based on a suitable representation of the workspace by adapting a numerical procedure that has been preliminarily outlined in [10] as based on Lee and Yang approach [11] for a binary representation of a scanned mobility of input joints. The complexity of workspace evaluation can be simplified by using suitable volumes that represent the workspace. The numerical approximation using simple geometry leads to a fast computation for workspace evaluation.

The algorithm use a 3-dimensional matrix  $\mathbf{P}$  of entries  $\mathbf{P}_{ijk}$  in order to obtain a binary representation of the position workspace. If a generic grid pixel  $(i, j, k)$  of matrix  $\mathbf{P}$ , includes a reachable point then the corresponding element is set to 1, otherwise it is equal to 0.

In addition, a suitable reach frequency matrix

**D** of entries  $\mathbf{D}_{ijk}$  is defined to count the times that a corresponding point identified by  $\mathbf{P}_{ijk}$  is reached. Thus,  $\mathbf{D}_{ijk}$  can give a measure of the capability of the manipulator to reach a workspace point with several manipulator configurations. This can be considered as a measure for manipulator dexterity too.

Thus, a procedure for determination and evaluation of a manipulator position workspace can be summarized as follows:

1 Set maximum and minimum reaches along X, Y and Z axes; select proper resolution for the grids  $\Delta x$ ,  $\Delta y$  and  $\Delta z$ .

2 Define two 3-dimensional matrices **P** and **D** and set all entries equal to 0.

3 Determine the workspace by considering a suitable scanning of input joint angles, also by taking into account constraints that limit coordinates capabilities. Thus, determine x, y, z, which are the position coordinates of a reference point of the end-effector, for all manipulator configurations. Then, it is possible to compute the following:

3.1 Define the pixel coordinates as integer numbers i, j, k given by

$$i = \left\lfloor \frac{x + \Delta x}{\Delta x} \right\rfloor \quad j = \left\lfloor \frac{y + \Delta y}{\Delta y} \right\rfloor \quad k = \left\lfloor \frac{z + \Delta z}{\Delta z} \right\rfloor \quad (4)$$

where the operator  $\lfloor \cdot \rfloor$  denotes the floor function, that returns nearest integer less than or equal to the real-valued argument inside the brackets.

A node in the grid is indicated as  $H_{ijk}$  with i, j, k along X, Y and Z axes, respectively, as shown in Fig. 6.

3.2 Set the elements  $\mathbf{P}_{ijk}$ . A binary mapping for the workspace is given by

$$\mathbf{P}_{ijk} = \begin{cases} 0 & \text{if } H_{ijk} \notin W(H) \\ 1 & \text{if } H_{ijk} \in W(H) \end{cases} \quad (5)$$

where  $W(H)$  indicates the workspace region.

3.3 Set the elements  $\mathbf{D}_{ijk}$  to count each time the corresponding point  $H_{ijk}$  is reached. The binary mapping for repeatability is given by

$$\mathbf{D}_{ijk} = \mathbf{D}_{ijk} + 1 \quad (6)$$

each time the pixel  $\mathbf{P}_{ijk}$  is reached.

4 Evaluate workspace characteristics through the following steps:

4.1 The area for a generic cross-section in X-Y plane can be evaluated as

$$\text{Area} = \sum_{i=i_{\min}}^{i_{\max}} \sum_{j=j_{\min}}^{j_{\max}} \mathbf{P}_{ijk} \Delta x \Delta y \Big|_{k=k^*} \quad (7)$$

in which k is kept constant with a value  $k^*$

corresponding to the cross-section plane;  $i_{\min}$  and  $j_{\min}$  are the minimum values of the grid coordinates and  $i_{\max}$  and  $j_{\max}$  are the maximum values of the grid coordinates. The areas in other cross-sections can be evaluated by keeping constant the other indexes or a combination of them.

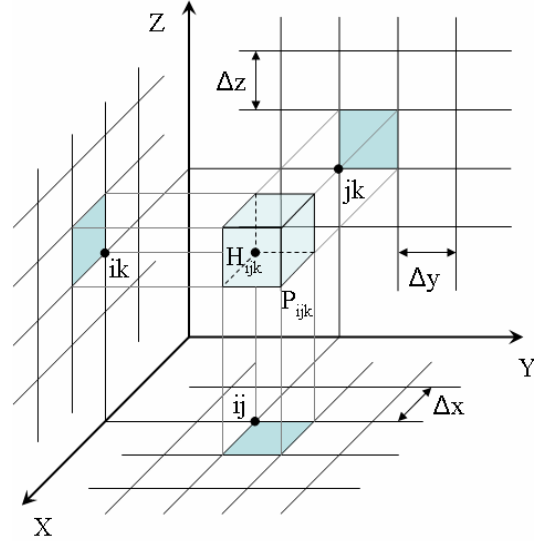


Fig. 6. A binary representation of a workspace pixel identified by  $\mathbf{P}_{ijk}$ .

4.2 The workspace volume can be evaluated as

$$\text{Vol} = \sum_{i=i_{\min}}^{i_{\max}} \sum_{j=j_{\min}}^{j_{\max}} \sum_{k=k_{\min}}^{k_{\max}} \mathbf{P}_{ijk} \Delta x \Delta y \Delta z \quad (8)$$

where  $i_{\min}$ ,  $j_{\min}$  and  $k_{\min}$  are the minimum values of the grid coordinates and  $i_{\max}$ ,  $j_{\max}$  and  $k_{\max}$  are the maximum values of the grid coordinates.

4.3 Evaluate the manipulator dexterity measure by using a frequency binary matrix through a procedure with Eq. (6).

Thus, matrix **P** will represent the position workspace and matrix **D** describes a repeatability measure.

#### 4. EFFECT OF LINK PARAMETERS ON WORKSPACE CHARACTERISTICS

In this section, several computations of the CaPaMan workspace are reported in order to characterize the workspace capability as function of design and operation parameters. The parameters investigated are

- $b_k$ , which is the length of the input crank;
- $\alpha_k$ , which is the input crank angle actuated by a DC motor, variable from the value  $\alpha_k$  min to  $\alpha_k$  max;
- $s_k$ , which is the stroke of the prismatic passive joint with range from  $s_k$  min to  $s_k$  max.

Table 2 show the range of design and operation parameters that have been investigated in this work. For each numerical simulation in the

analysis, one parameter has been changed and all the other parameters have been set to the default values with original design of CaPaMan, according to Table 1.

Table 2. Range of sizes and motion parameters for parametric study of CaPaMan.

	$b_k$ and $d_k$ [mm]	$\alpha_{k,min}$ [deg]	$\alpha_{k,max}$ [deg]	$s_{k,min}$ [mm]	$s_{k,max}$ [mm]
Range	40 to 140	0 to 50	130 to 180	-75 to -25	25 to 75
Step	5	2.5	2.5	2.5	2.5

#### 4.1 Effect of link parameter $b_k$

The following results show the effects of design parameter  $b_k$  on workspace volume, cross sections area and dexterity capability. In particular the  $b_k$  parameter analysis has been carried out with the following conditions:

- $b_1 = b_2$ , which are the lengths of the input cranks 1 and 2;
- $b_3$ , which is the length of the input crank 3.

The study has been carried out by evaluating workspace characteristics for several values of  $b_1$ ,  $b_2$  and  $b_3$ . The range of  $b_k$  parameter starts from 40 mm up to 140 mm. The parameterization step used for the investigation has been set equal to 5 mm.

An example has been reported with design parameter  $b_1 = b_2 = 100$  mm and  $b_3 = 50$  mm, and it is referred as example #1, in order to show how the workspace has changed shape and characteristics.

Figures 7 to 9 show the position workspace characteristics for the example #1.

Figures 10 to 12 show the relationship between main workspace characteristics as function of  $b_k$ . Figure 10 shows the volume evaluation, and it is useful to recognize that the maximum volume can be obtained for maximum values of  $b_1$ ,  $b_2$  and  $b_3$ . The effects of  $b_1$ ,  $b_2$  and  $b_3$  on the cross sections area are similar, since little numerical differences are imputable to the discretization. Indeed, as reported in Fig. 11, some cross sections have the maximum area when  $b_1$ ,  $b_2$  and  $b_3$  have the maximum value. Figure 12 shows the maximum dexterity as corresponding to the cross sections.

Two particular points are marked in Figs. 10, 11 and 12. Full square recognize the prototype design parameter, whereas the circle point identifies the above-mentioned example #1.

The results of this numerical analysis show that the workspace volume strongly depends on  $b_k$  values, even with unsymmetrical designs. However, differences in  $b_k$  sizes give loss and distortion of symmetrical shape of the workspace figure and dexterity characteristics.

#### 4.2 Effect of link parameters $\alpha_k$

The following results show the effects of motion parameter  $\alpha_k$  on workspace volume, cross

sections area and dexterity capability. This motion parameter has two limits:

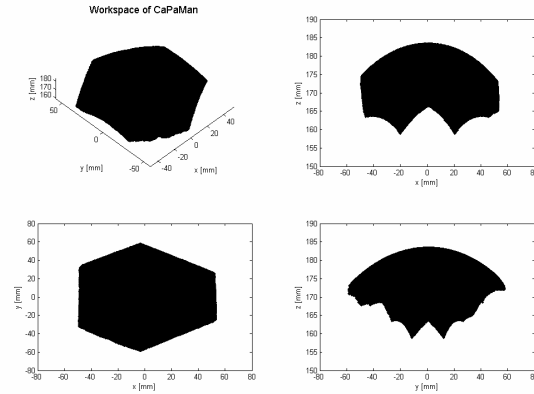


Fig. 7. A 3-D representation with Cartesian projections of CaPaMan position workspace with design parameters  $b_1 = b_2 = 100$  mm and  $b_3 = 50$  mm.

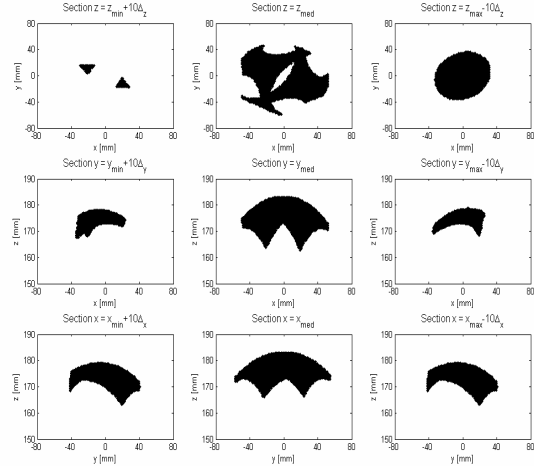


Fig. 8. Workspace cross sections of CaPaMan in Fig. 7 with design parameters  $b_1 = b_2 = 100$  mm and  $b_3 = 50$  mm.

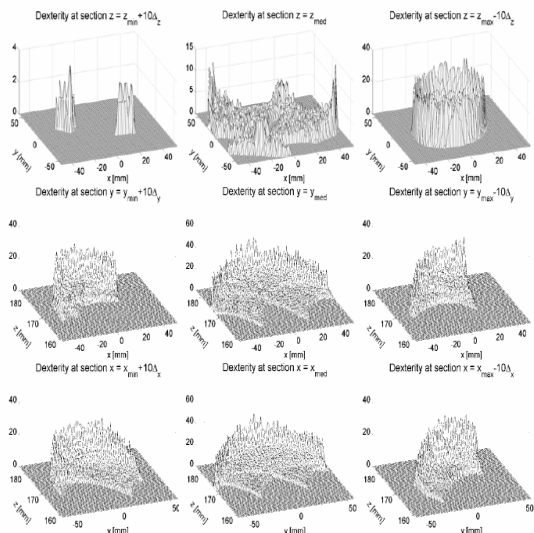


Fig. 9. Dexterity map for workspace cross-sections of CaPaMan in Fig. 8 with design parameters  $b_1 = b_2 = 100$  mm and  $b_3 = 50$  mm.

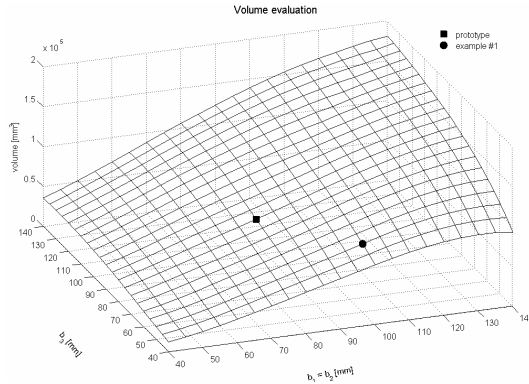


Fig. 10. Evaluation of CaPaMan workspace volume as function of design parameters  $b_1 = b_2$  and  $b_3$  (■ prototype; ● example #1).

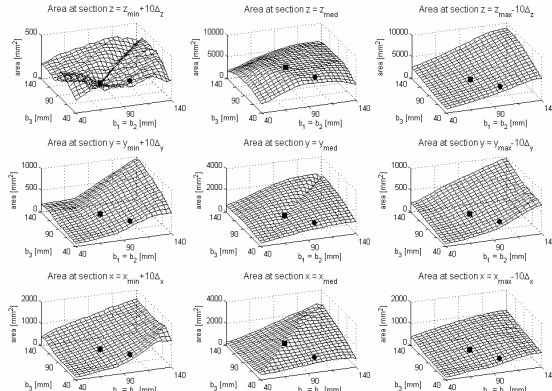


Fig. 11. Evaluation of CaPaMan workspace cross sections area as function of design parameters  $b_1 = b_2$  and  $b_3$  (■ prototype; ● example #1).

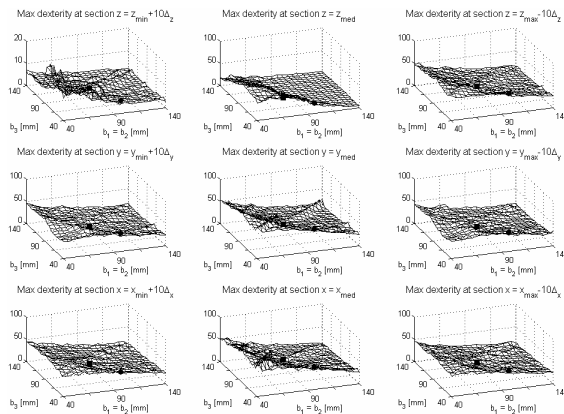


Fig. 12. Evaluation of CaPaMan workspace cross-sections max dexterity as function of design parameters  $b_1 = b_2$  and  $b_3$  (■ prototype; ● example #1).

- $\alpha_k$  min, which is the minimum value reachable by  $\alpha_k$ ;

- $\alpha_k$  max, which is the maximum value reachable by  $\alpha_k$ .

The study has been carried out by evaluating workspace characteristics for several values of  $\alpha_k$  min and  $\alpha_k$  max. The range of  $\alpha_k$  min parameter starts from 0 degrees up to 50 degrees. The range of  $\alpha_k$  max parameter starts from 130 degrees up to 180 degrees. The parameterization step for the investigation has been set equal to 2.5 degrees.

An example has been reported with motion parameter  $\alpha_k$  min = 5 degrees and  $\alpha_k$  max = 175 degrees, and it referred as example #2, in order to show how the workspace has changed in shape and characteristics.

Figures 13 to 15 show the workspace characteristics for the example #2.

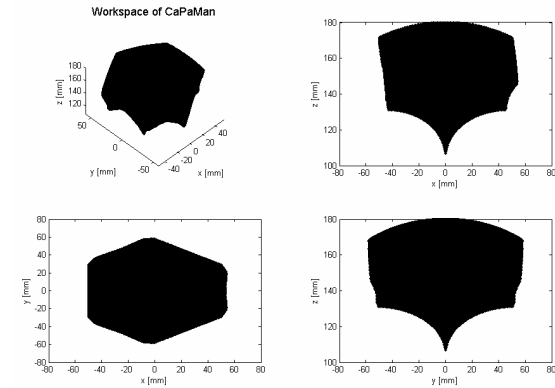


Fig. 13. A 3-D representation with Cartesian projections of CaPaMan position workspace with motion parameters  $\alpha_k$  min = 5 deg and  $\alpha_k$  max = 175 deg.

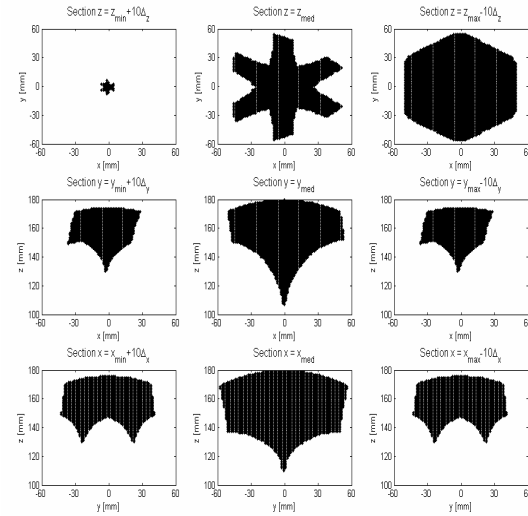


Fig. 14. Workspace cross sections of CaPaMan in Fig. 13 with motion parameters  $\alpha_k$  min = 5 deg and  $\alpha_k$  max = 175 deg.

Figures 16 to 18 show the relationship between main workspace characteristics as function of  $\alpha_k$  min and  $\alpha_k$  max. Figure 16 shows the volume

evaluation, and it is useful to recognize that the greater volume can be obtained for the minimum value of  $\alpha_k$  min and maximum value of  $\alpha_k$  max. The effects of  $\alpha_k$  min and  $\alpha_k$  max on the cross sections area are different. Indeed, as reported in Fig. 17, some cross sections have the maximum area when  $\alpha_k$  min +  $\alpha_k$  max = 180 degrees. Figure 18 shows the maximum dexterity as corresponding to the cross sections. Two particular points are marked in Figs. 16 to 18. A full square recognize the prototype default parameter, whereas the circle point identifies the example #2.

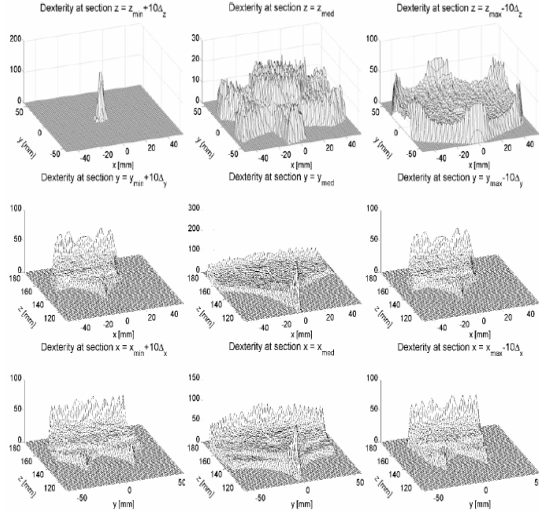


Fig. 15. Dexterity map for workspace cross sections of CaPaMan in Fig. 14 with motion parameters  $\alpha_k$  min = 5 deg and  $\alpha_k$  max = 175 deg.

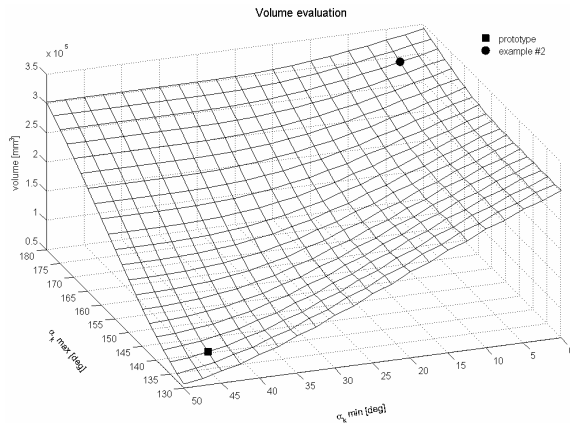


Fig.16. Evaluation of CaPaMan workspace volume as function of motion parameters  $\alpha_k$  min and  $\alpha_k$  max (■ prototype; ● example #2).

Moreover, in this work different values have been analyzed for  $\alpha_k$  min and  $\alpha_k$  max in each limb. In particular the  $\alpha_k$  min parameter has been split in two parameters in order to study the main possible combinations of motion:

- $\alpha_1$  min =  $\alpha_2$  min, which is the minimum value reachable by  $\alpha_1$  and  $\alpha_2$ ;

- $\alpha_3$  min, which is the minimum value reachable for  $\alpha_3$ .

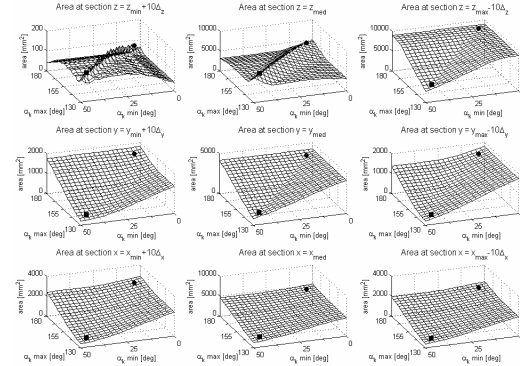


Fig. 17. Evaluation of CaPaMan workspace cross sections area as function of motion parameters  $\alpha_k$  min and  $\alpha_k$  max (■ prototype; ● example #2).

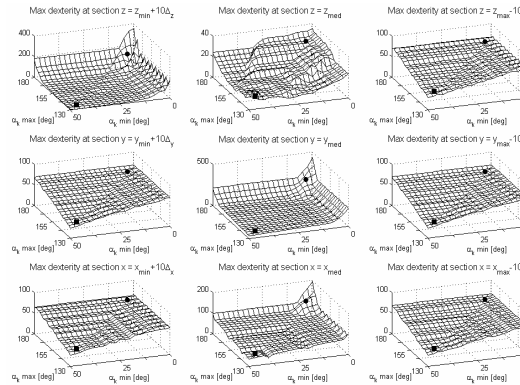


Fig. 18. Evaluation of CaPaMan workspace cross sections max dexterity as function of motion parameters  $\alpha_k$  min and  $\alpha_k$  max (■ prototype; ● example #2).

The range of parameters  $\alpha_1$  min,  $\alpha_2$  min and  $\alpha_3$  min starts from 0 degrees up to 50 degrees. The parameterization step for the investigation has been set equal to 2.5 degrees.

An example has been reported with motion parameter  $\alpha_1$  min =  $\alpha_2$  min = 25 degrees and  $\alpha_3$  min = 10 degrees, and this example will be referred to as example #3, in order to show how the workspace has changed in shape and characteristics.

Figures 19 to 21 show the workspace characteristics for the example #3.

Figures 22 to 24 show the relationship between main workspace characteristics as function of  $\alpha_1$  min,  $\alpha_2$  min and  $\alpha_3$  min. Figure 22 shows the volume evaluation, and it is useful to recognize that the maximum volume can be obtained for minimum values of  $\alpha_1$  min,  $\alpha_2$  min and  $\alpha_3$  min. Figure 23 shows main cross sections area. Figure 35 shows the maximum dexterity as corresponding to the cross sections.

In Figs. 22 to 24 two particular points have been highlighted. A full square recognize the



prototype default parameters, whereas the circle point identifies example #3.

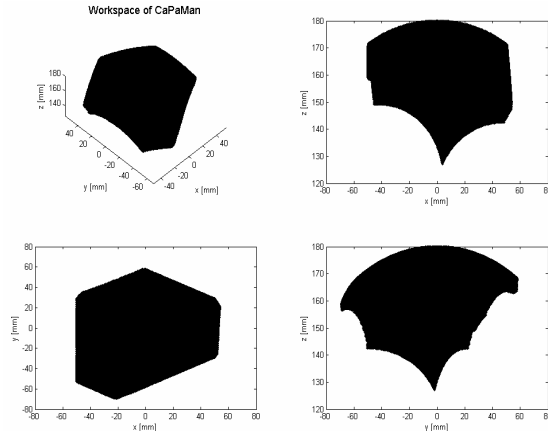


Fig. 19. A 3-D representation with Cartesian projections of CaPaMan position workspace with motion parameters  $\alpha_1 \min = \alpha_2 \min = 25$  deg and  $\alpha_3 \min = 10$  deg.

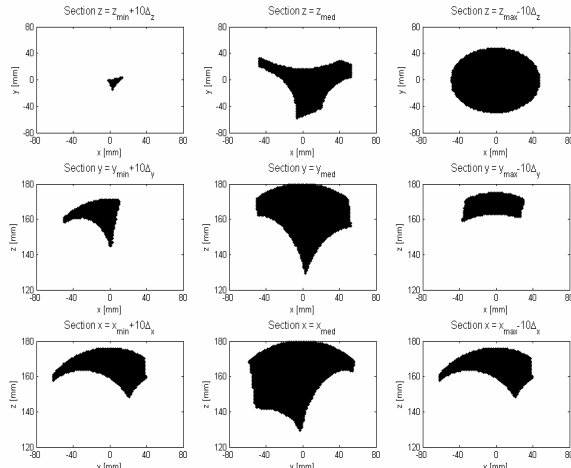


Fig. 20. Workspace cross sections of CaPaMan in Fig. 19 with motion parameters  $\alpha_1 \min = \alpha_2 \min = 25$  deg and  $\alpha_3 \min = 10$  deg.

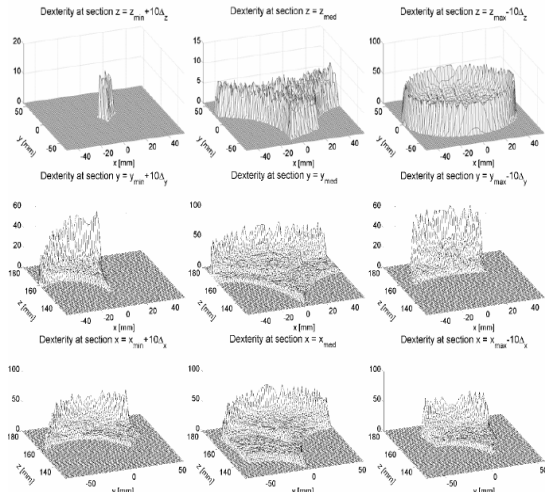


Fig. 21. Dexterity map for workspace cross sections of CaPaMan in Fig. 20 with motion parameters  $\alpha_1 \min = \alpha_2 \min = 25$  deg and  $\alpha_3 \min = 10$  deg.

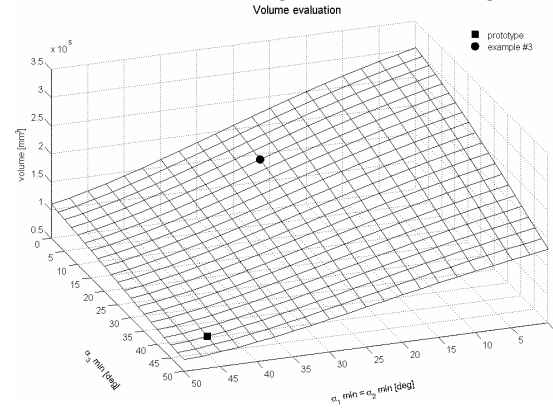


Fig. 22. Evaluation of CaPaMan workspace volume as function of motion parameters  $\alpha_1 \min = \alpha_2 \min$  and  $\alpha_3 \min$  (■ prototype; ● example #3).

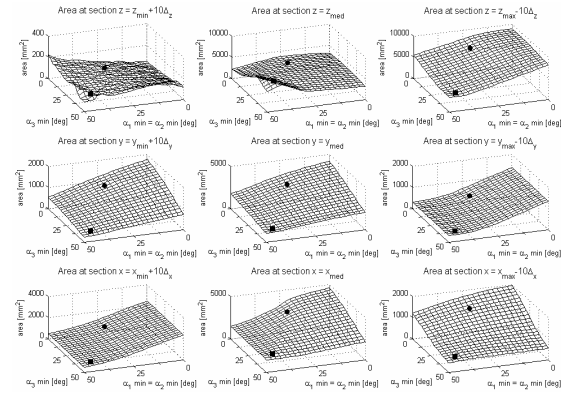


Fig. 23. Evaluation of CaPaMan workspace cross-sections area as function of motion parameters  $\alpha_1 \min = \alpha_2 \min$  and  $\alpha_3 \min$  (■ prototype; ● example #3).

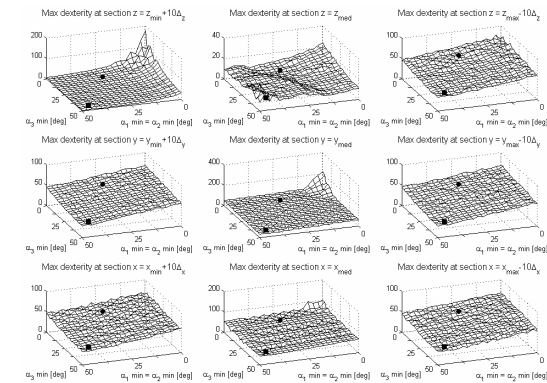


Fig. 24. Evaluation of CaPaMan workspace cross-sections max dexterity as function of motion parameters  $\alpha_1 \min = \alpha_2 \min$  and  $\alpha_3 \min$  (■ prototype; ● example #3).

The  $\alpha_k \max$  parameter has been split in two parameters:

- $\alpha_1 \max = \alpha_2 \max$ , which is the maximum value reachable by  $\alpha_1$  and  $\alpha_2$ ;
- $\alpha_3 \max$ , which is the maximum value reachable by  $\alpha_3$ .

The range of parameter  $\alpha_1 \max$ ,  $\alpha_2 \max$  and  $\alpha_3 \max$  starts from 130 degrees up to 180 degrees. The parameterization step for the investigation has been set equal to 2.5 degrees.

An example has been reported with motion parameter  $\alpha_1 \max = \alpha_2 \max = 170$  degrees and  $\alpha_3 \max = 175$  degrees, and this example will be referred to as example #4, in order to show the effects of this parameter on the workspace shape and characteristics.

Figures 25 to 27 show the workspace characteristics for the example #4.

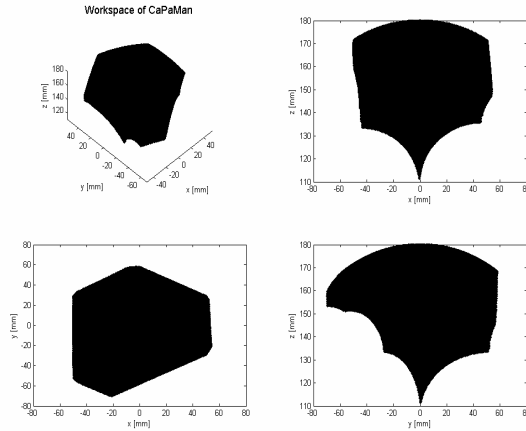


Fig. 25. A 3-D representation with Cartesian projections of CaPaMan position workspace with motion parameters  $\alpha_1 \max = \alpha_2 \max = 170$  deg and  $\alpha_3 \max = 175$  deg.

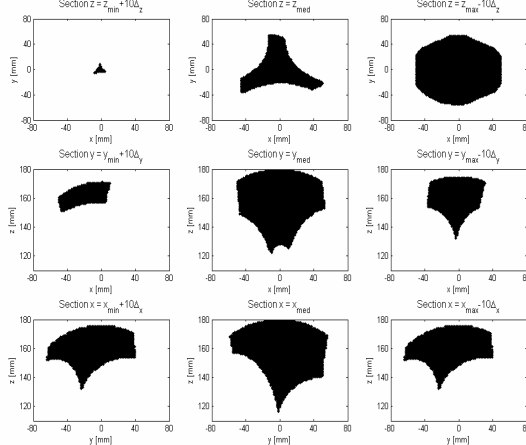


Fig. 26. Workspace cross sections of CaPaMan in Fig. 25 with motion parameters  $\alpha_1 \max = \alpha_2 \max = 170$  deg and  $\alpha_3 \max = 175$  deg.

Figures 28 to 30 show the relationship between main workspace characteristics as function of  $\alpha_1 \max$ ,  $\alpha_2 \max$  and  $\alpha_3 \max$ . Figure 28 shows the volume evaluation, and it is useful to recognize that the maximum volume can be obtained for maximum

values of  $\alpha_1 \max$ ,  $\alpha_2 \max$  and  $\alpha_3 \max$ . Figure 29 shows main cross sections area. Figure 30 shows the maximum dexterity as corresponding to the cross sections.

Figures 28 to 30 contain two highlighted particular points. A full square recognize the prototype default parameter, whereas the circle point identifies example #4.

The workspace shows considerable design sensitivity as function of the values of  $\alpha_k$ , both in term of shape modification and volume value. In addition, the input range affects the workspace characteristics, even with the values of  $\alpha_k \min$  and  $\alpha_k \max$ . Unsymmetrical operation data are even more influent in the distortion of the workspace shape and alteration of dexterity maps, but after certain values of  $\alpha_k$  differences.

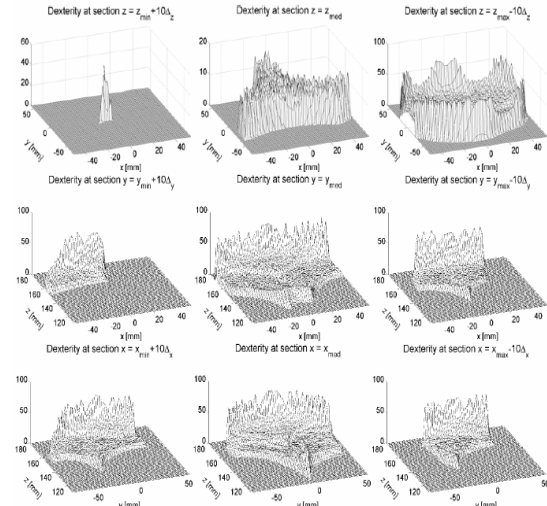


Fig. 27. Dexterity map for workspace cross sections of CaPaMan in Fig. 26 with motion parameters  $\alpha_1 \max = \alpha_2 \max = 170$  deg and  $\alpha_3 \max = 175$  deg.

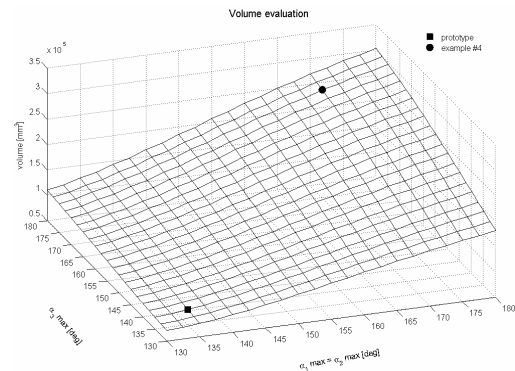


Fig. 28. Evaluation of CaPaMan workspace volume as function of motion parameters  $\alpha_1 \max = \alpha_2 \max$  and  $\alpha_3 \max$  (■ prototype; ● example #4).

### 4.3 Effect of link parameters $s_k$

The following results show the effects of motion parameter  $s_k$  on workspace volume, cross

sections area and dexterity capability. This design parameter has two limits:

- $s_k$  min, which is the minimum value reachable by  $s_k$ ;
- $s_k$  max, which is the maximum value reachable by  $s_k$ .

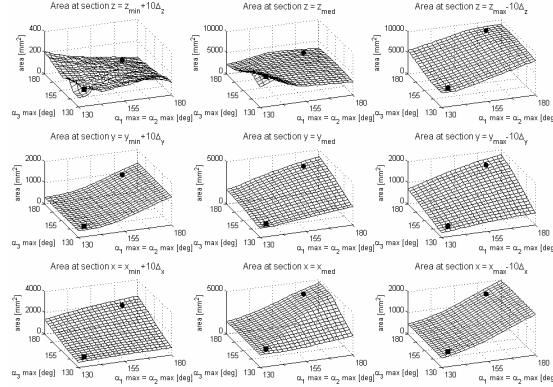


Fig. 29. Evaluation of CaPaMan workspace cross sections area as function of motion parameters  $\alpha_1$  max =  $\alpha_2$  max and  $\alpha_3$  max (■ prototype; ● example #4).

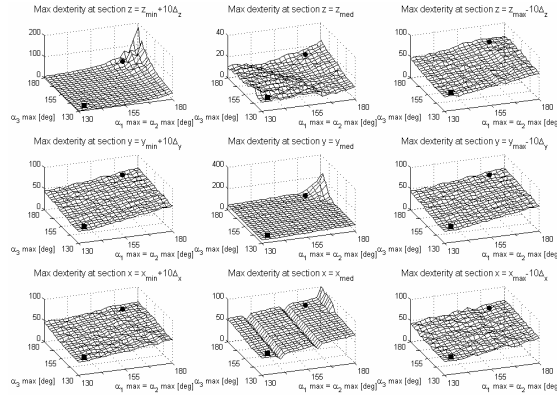


Fig. 30. Evaluation of CaPaMan workspace cross sections max dexterity as function of motion parameters  $\alpha_1$  max =  $\alpha_2$  max and  $\alpha_3$  max (■ prototype; ● example #4).

The study has been carried out by evaluating workspace characteristics for several values of  $s_k$  min and  $s_k$  max. The range of  $s_k$  min parameter starts from -75 mm up to -25 mm. The range of  $s_k$  max parameter starts from 25 mm up to 75 mm. The parameterization step for the investigation has been set equal to 2.5 mm. An example with design parameter  $s_k$  min = -70 and  $s_k$  max = 70 mm, and this example will be referred to as example #5, has been reported in order to show how the workspace has changed in shape and characteristics.

Figures 31 to 33 show the workspace characteristics for the example #5.

Figures 34 to 36 show the relationship between main workspace characteristics as function of  $s_k$  min and  $s_k$  max. Figure 34 shows the volume evaluation, and it is useful to recognize that the

maximum volume can be obtained for minimum value of  $s_k$  min and maximum value of  $s_k$  max. Figure 35 shows the cross sections area. Figure 36 shows the maximum dexterity for each cross sections.

In Figs. 34 to 36 have been highlighted two particular points. A full square recognize the prototype default parameter, whereas the circle point identifies the example #5.

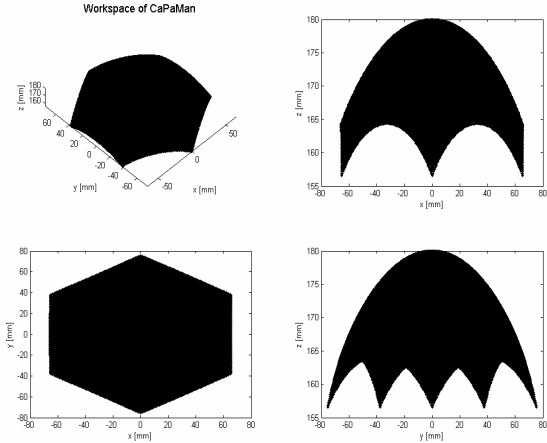


Fig.31. A 3-D representation with Cartesian projections of CaPaMan position workspace with design parameters  $s_k$  min = -70 mm and  $s_k$  max = 70 mm.

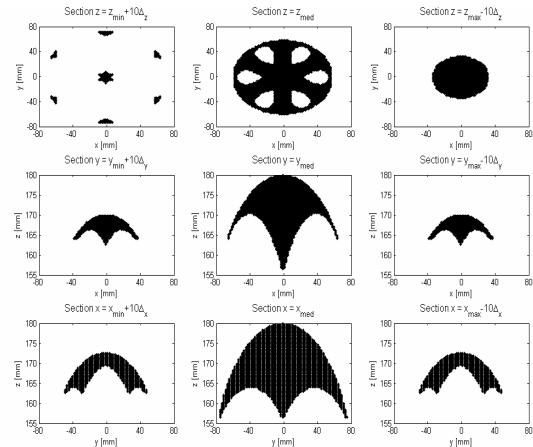


Fig. 32. Workspace cross-sections of CaPaMan in Fig. 31 with design parameters  $s_k$  min = -70 mm and  $s_k$  max = 70 mm.

Moreover, in this work different values have been analyzed for of  $s_k$  min and  $s_k$  max in each limb. In particular the  $s_k$  min parameter has been split in two parameters in order to study the main possible combinations of motion:

- $s_1$  min =  $s_2$  min, which is the minimum value reachable by  $s_1$  and  $s_2$ ;
- $s_3$  min, which is the minimum value reachable by  $s_3$ .

The range of parameters  $s_1$  min,  $s_2$  min and  $s_3$  min starts from -75 mm up to -25 mm. The

parameterization step for the investigation has been set equal to 2.5 mm.

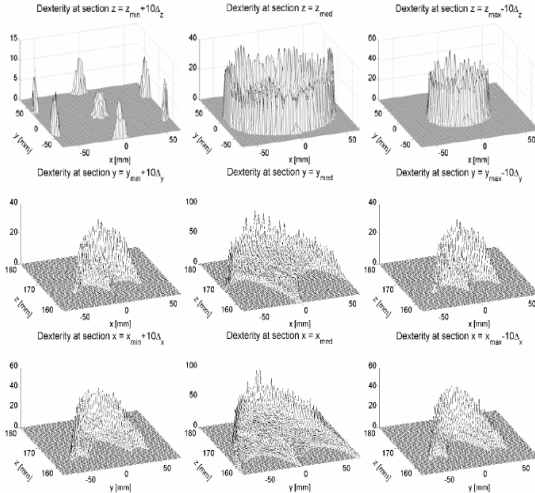


Fig. 33. Dexterity map for workspace cross sections of CaPaMan in Fig. 32 with design parameters  $s_k$  min = -70 mm and  $s_k$  max = 70 mm.

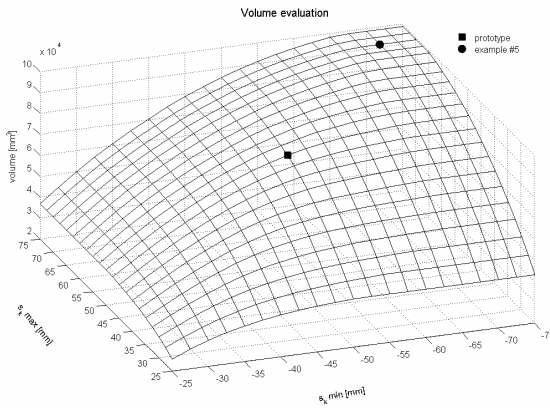


Fig. 34. Evaluation of CaPaMan workspace volume as function of design parameters  $s_k$  min and  $s_k$  max (■ prototype; ● example #5).

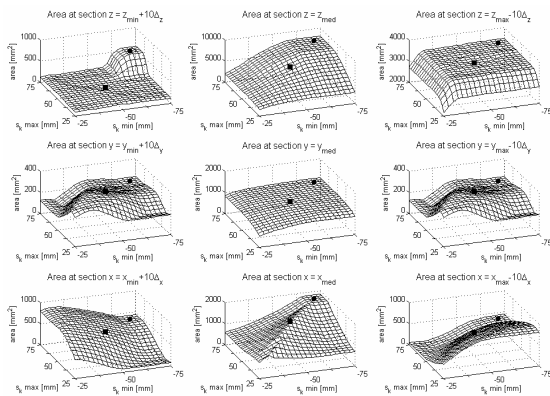


Fig. 35. Evaluation of CaPaMan workspace cross sections area as function of design parameters  $s_k$  min and  $s_k$  max (■ prototype; ● example #5).

An example with motion parameter  $s_1$  min =  $s_2$  min = -30 mm and  $s_3$  min = -70 mm has been reported, and it is referred as example #6, in order to show how the workspace has changed in shape and characteristics.

Figures 37 to 39 show the workspace characteristics for the example #6.

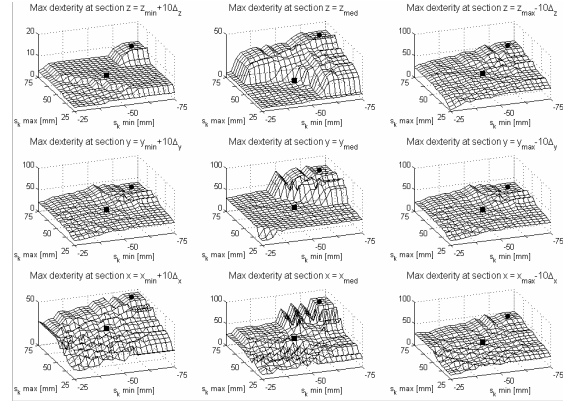


Fig. 36. Evaluation of CaPaMan workspace cross-sections max dexterity as function of design parameters  $s_k$  min and  $s_k$  max (■ prototype; ● example #5).

Figures 40 to 42 show the relationship between main workspace characteristics as function of  $s_1$  min,  $s_2$  min and  $s_3$  min. Figure 40 shows the volume evaluation, and it is useful to recognize that the maximum volume can be obtained for minimum values of  $s_1$  min,  $s_2$  min and  $s_3$  min. Figure 41 shows main cross sections area. Figure 42 shows the maximum dexterity as corresponding to the cross sections.

In Figs. 40 to 42 two particular points have been highlighted. A full square matches the prototype default parameters, whereas the circle point identifies example #6.

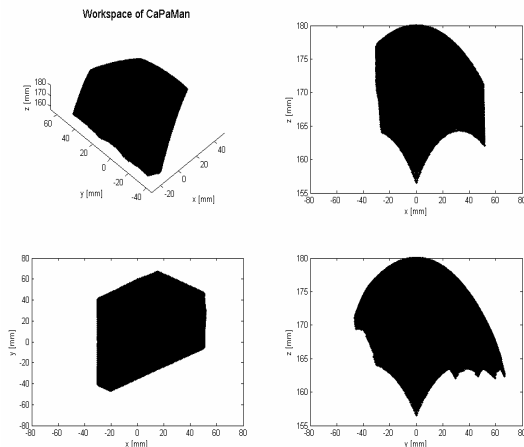


Fig. 37. A 3-D representation with Cartesian projections of CaPaMan position workspace with design parameters  $s_1$  min =  $s_2$  min = -30

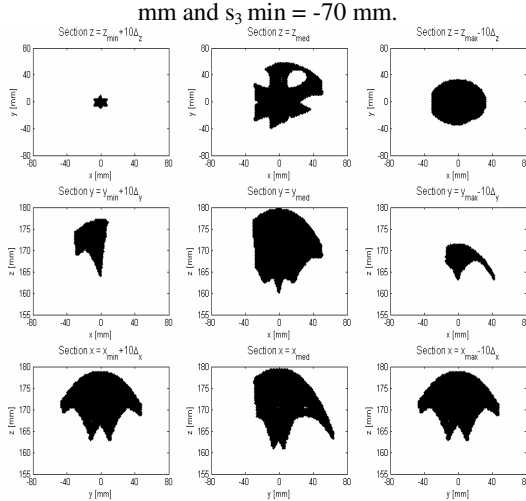


Fig. 38. Workspace cross sections of CaPaMan in Fig. 37 with design parameters  $s_1 \min = s_2 \min = -30$  mm and  $s_3 \min = -70$  mm.

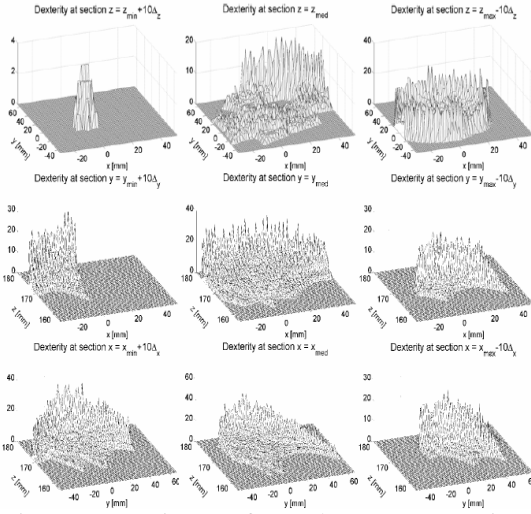


Fig. 39. Dexterity map for workspace cross sections of CaPaMan in Fig. 38 with design parameters  $s_1 \min = s_2 \min = -30$  mm and  $s_3 \min = -70$  mm.

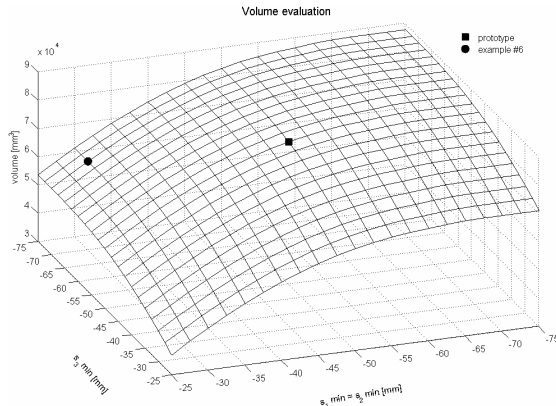


Fig. 40. Evaluation of CaPaMan workspace volume as function of design parameters  $s_1 \min = s_2 \min$  and  $s_3 \min$  (■ prototype; ● example #6).

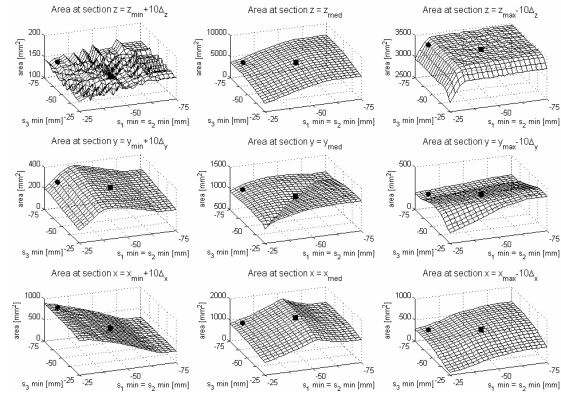


Fig. 41. Evaluation of CaPaMan workspace cross sections area as function of design parameters  $s_1 \min = s_2 \min$  and  $s_3 \min$  (■ prototype; ● example #6).

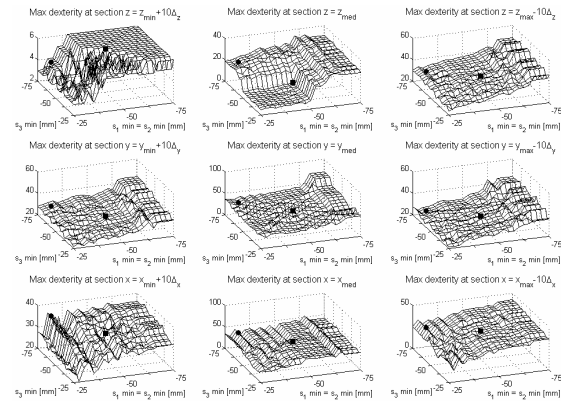


Fig. 42. Evaluation of CaPaMan workspace cross sections max dexterity as function of design parameters  $s_1 \min = s_2 \min$  and  $s_3 \min$  (■ prototype; ● example #6).

The  $s_k \max$  parameter has been split in two parameters:

- $s_1 \max = s_2 \max$ , which is the maximum value reachable by  $s_1$  and  $s_2$ ;
- $s_3 \max$ , which is the maximum value reachable by  $s_3$ .

The range of parameter  $s_1 \max$ ,  $s_2 \max$  and  $s_3 \max$  starts from 25 mm up to 75 mm. The parameterization step for the investigation has been set equal to 2.5 mm.

An example with motion parameter  $s_1 \max = s_2 \max = 50$  mm and  $s_3 \max = 70$  mm has been reported, and this example will be referred to as example #7, in order to show the effects of this parameter on the workspace shape and characteristics.

Figures 43 to 45 show the workspace characteristics for the example #7.

Figures 46 to 48 show the relationship between main workspace characteristics as function of  $s_1 \max$ ,  $s_2 \max$  and  $s_3 \max$ . Figure 46 shows the volume evaluation, and it is useful to admit that the maximum volume can be obtained for maximum values of  $s_1 \max$ ,  $s_2 \max$  and  $s_3 \max$ . Figure 47 shows

main cross sections area. Figure 48 shows the maximum dexterity as corresponding to the cross sections.

Figures 46 to 48 contain two highlighted particular points. A full square matches the prototype default parameter, whereas the circle point identifies example #7.

The effects of the stroke size in the prismatic guide is relevant as intuitively expected, both in term of values and shape of workspace characteristics, mainly for large values of stroke. In addition, workspace characteristics are calculated as very sensitive in the difference of three strokes, both in terms of ranges and limit values (min and max).

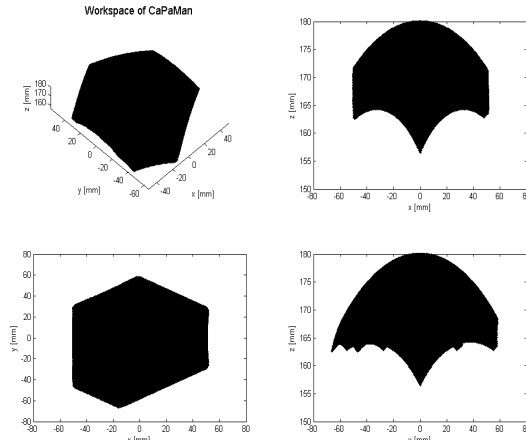


Fig. 43. 3-D representation with Cartesian projections of CaPaMan position workspace with design parameters  $s_1 \text{ max} = s_2 \text{ max} = 50 \text{ mm}$  and  $s_3 \text{ max} = 70 \text{ mm}$ .

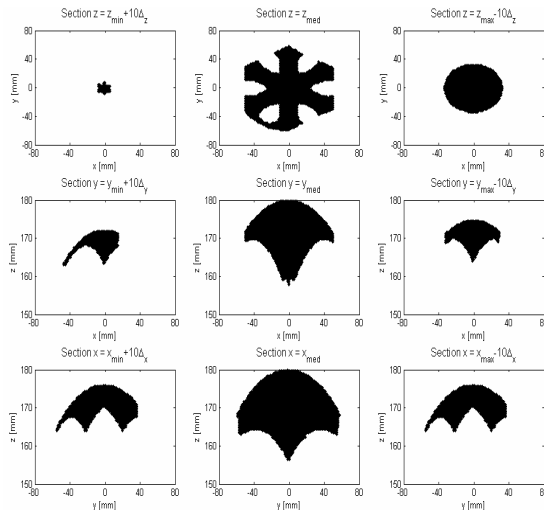


Fig. 44. Workspace cross sections of CaPaMan with design parameters  $s_1 \text{ max} = s_2 \text{ max} = 50 \text{ mm}$  and  $s_3 \text{ max} = 70 \text{ mm}$ .

Summarizing, the proposed numerical parametric study shows that the CaPaMan position workspace is characterized by a bulk shape figure

with strong symmetry that can be completely lost

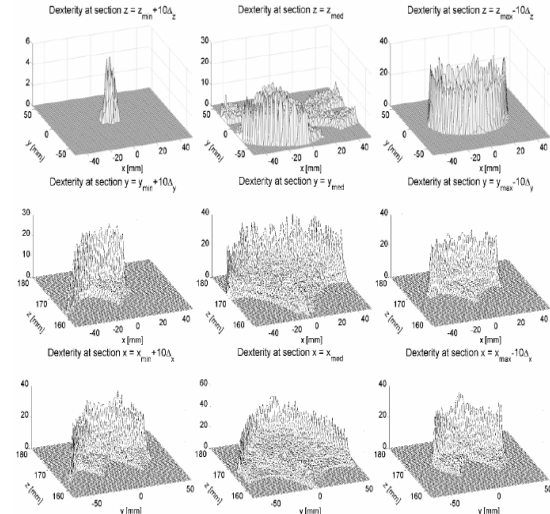


Fig. 45. Dexterity map for workspace cross sections of CaPaMan with design parameters  $s_1 \text{ max} = s_2 \text{ max} = 50 \text{ mm}$  and  $s_3 \text{ max} = 70 \text{ mm}$ .

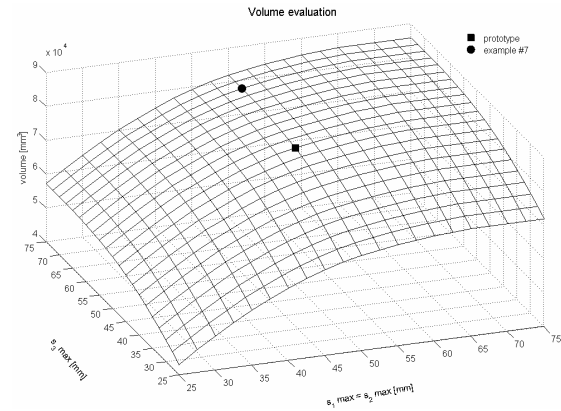


Fig. 47. Evaluation of CaPaMan workspace volume with respect to design parameters  $s_1 \text{ max} = s_2 \text{ max}$  and  $s_3 \text{ max}$  (■ prototype; ● example #7).

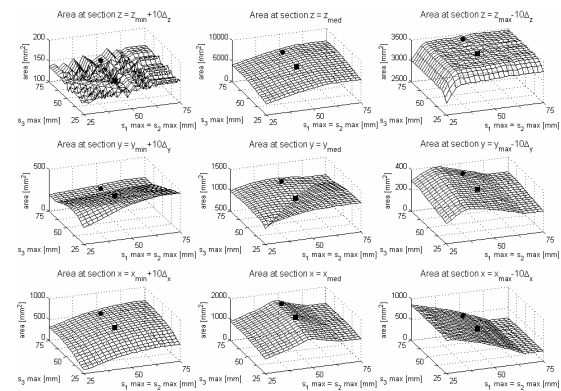


Fig. 47. Evaluation of CaPaMan workspace cross sections area with respect to design parameters  $s_1 \text{ max} = s_2 \text{ max}$  and  $s_3 \text{ max}$  (■ prototype; ● example #7).

only with strong asymmetry in the design parameters.

A certain sensitivity has been computed even for small design errors, that nevertheless do not modify significantly the position workspace characteristics of CaPaMan.

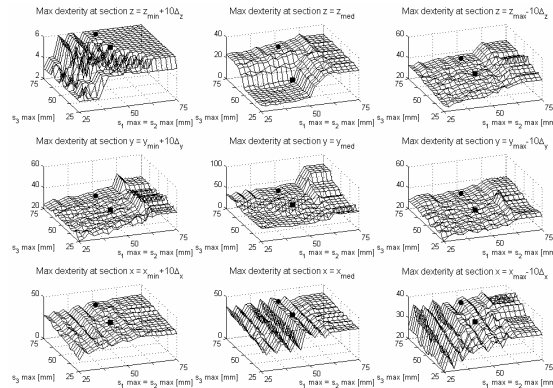


Fig. 48. Evaluation of CaPaMan workspace cross sections max dexterity with respect to design parameters  $s_1 \max = s_2 \max$  and  $s_3 \max$  (■ prototype; ● example #7).

## 6. CONCLUSIONS

In this paper, we have presented a numerical investigation of the effects of design parameters for CaPaMan architecture on its workspace characteristics. The peculiar topology and functional aspects are outlined through several plots that are obtained by means of a suitable analysis. The proposed parametric study has shown that the position workspace of CaPaMan is characterized by shape and values that are not significantly affected by small errors in design and operation parameters, where as it can suffer relevant loss of symmetrical properties for large variations of design sizes.

## REFERENCES

- [1] **R. E. Stammer, L. W. Tsai, G. C. Walsh**, *Optimization of a three dof translational platform for well-conditioned workspace*. Technical Research Report, 1997.
- [2] **M. Ceccarelli, E. Ottaviano**, *A workspace evaluation of an eclipse robot*. Robotica 20 (2002) 299-313.
- [3] **C. M. Gosselin, M. Guilloit**, *The synthesis of manipulators with prescribed workspace*. Journal of Mechanical Design 113 (1991) 451-455.
- [4] **O. Ma, J. Angeles**, *Optimum architecture design of platform manipulators*. Proc. of ICRA 91 - The Int. Conference on Robotics and Automation (1991) 1130-1135.
- [5] **C. Gosselin, J. Angeles**, *A global performance index for the kinematic optimization of robotic manipulators*. ASME Journal of Mechanical Design 113, (1991) 220-226.
- [6] **V. Parenti-Castelli, R. Di Gregorio**, *Workspace and optimal design of pure translation parallel manipulator*. XIV Italian National Congress AIMETA '99, Como, 1999, paper No.65.
- [7] **M. Ceccarelli**, *A new 3 dof spatial parallel mechanism*. Mechanism and Machine Theory 32 (8) (1997) 895-902.
- [8] **E. Ottaviano, M. Ceccarelli, G. Castelli**, *Experimental results of a 3-dof parallel manipulator as an earthquake motion simulator*. ASME IDECT '04 Mechanisms and Robotics Conference, Salt Lake City, 2004, Paper DETC2004-57075.
- [9] **G. Castelli, E. Ottaviano, M. Ceccarelli**, *A fairly general algorithm to evaluate workspace characteristics of serial and parallel manipulators*. Mechanics Based Design of Structures and Machines (2008) (in print).
- [10] **M. Ceccarelli, E. Gabriele**, *Determining primary and secondary workspaces of industrial robots*. Proceedings of the 4th International Workshop on Robotics in Alpe-Adria Region, Portsach, 1995, (2) 259-262.
- [11] **T.W. Lee, D.C.H. Yang**, *On the evaluation of manipulator workspace*. ASME Journal of Mechanisms Transmissions, and Automation in Design 105 (1983) 70-77.